Int. J. Devl Neuroscience 27 (2009) 329–336

Contents lists available at ScienceDirect

International Journal of Developmental Neuroscience

journal homepage: www.elsevier.com/locate/ijdevneu

The developing and restructuring superior cervical ganglion of guinea pigs (*Cavia porcellus* var. *albina*)

Cauê Pereira Toscano [a], Mariana Pereira de Melo [b], Júlia Maria Matera [c], Andrzej Loesch [d], Antonio Augusto Coppi Maciel Ribeiro [a,*]

[a] *Laboratory of Stochastic Stereology and Chemical Anatomy (LSSCA), Department of Surgery, College of Veterinary Medicine, University of São Paulo (USP), São Paulo, Brazil*
[b] *Department of Statistics, Institute of Mathematics and Statistics, University of São Paulo, Brazil*
[c] *Department of Surgery, College of Veterinary Medicine, University of São Paulo (USP), São Paulo, Brazil*
[d] *Research Department of Inflammation, University College London Medical School, Royal Free Campus, London, UK*

ARTICLE INFO

Article history:
Received 3 December 2008
Received in revised form 5 February 2009
Accepted 15 March 2009

Keywords:
SCG
Post-natal development
Design-based stereology
Guinea pigs
Rodents

ABSTRACT

Post-natal development comprises both maturation (from newborn to adult) and ageing (from adult to senility) and, during this phase, several adaptive mechanisms occur in sympathetic ganglia, albeit they are not fully understood. Therefore, the present study aimed at detecting whether post-natal development would exert any effect on the size and number of a guinea pig's superior cervical ganglion (SCG) neurons. Twenty right SCGs from male subjects were used at four ages, i.e. newborn (7 days), young (30 days), adult (7 months) and old animals (50 months). Using design-based stereological methods the volume of ganglion and the total number of mononucleate and binucleate neurons were estimated. Furthermore, the mean perikaryal volume of mononucleate and binucleate neurons was estimated using the vertical nucleator. The main findings of this study were a combination of post-natal-dependent increases and decreases in some variables: (i) 27% increase in ganglion volume, (ii) 24% and 43% decreases in the total number of mono and binucleate neurons, respectively, and (iii) 27.5% and 40% decreases in the mean perikaryal volume of mono and binucleate neurons, respectively. Despite the fall in neuron numbers found here, post-natal development is not only associated with neuron loss, but also embraces other structural adaptive mechanisms, which are discussed in this paper.

1. Introduction

Post-natal development comprises two phases, i.e. maturation (from newborn to adult) and ageing (from adult to senility), and several adaptive mechanisms occur in sympathetic ganglia, albeit there is still a dearth of knowledge of them (Finch, 1993; Vega et al., 1993). Ageing may be accompanied by changes in cellular functions and the occurrence of possible degenerative processes. For instance, in the central nervous system (CNS), neuronal loss and either neuronal atrophy or hypertrophy are the most widely reported ageing-related changes (Cabello et al., 2002).

These claims are, however, controversial and doubtful since structural differences in various constituents of the nervous system have been reported in a huge variety of animal species (Finch, 1993; Vega et al., 1993). For instance, the number of neurons in the hypogastric ganglion of rats of 24 months old is higher than in rats of 4 months old (Warburton and Santer, 1997) and it is higher in the dorsal root ganglia (DRG) of rats of 80 days old than in rats of 11 days old (Popken and Farel, 1997).

Several hypotheses for a differential (earlier or later) maturation of certain nervous system structures have been suggested. For example, Farel (2003) argued that the post-natal increase in the number of neurons in the rat's DRG was not associated with a possible neurogenesis, but perhaps with a late maturation or incomplete differentiation, causes of which remain unclear. On the other hand, recent publications describing binucleate neurons in the superior cervical ganglion (SCG) of adult wild rodents such as capybaras (Ribeiro et al., 2004; Ribeiro, 2006) and in the coeliac ganglion of adult lagomorphs (rabbits) (Sasahara et al., 2003), add further fuel to the notion that a post-natal neurogenesis may indeed exist in sympathetic ganglia.

In the light of this, the main aim of this study was to investigate whether maturation and ageing would affect the number and size of binucleate and mononucleate SCG neurons in guinea pigs. In order to achieve that three different methodological approaches were used, i.e. anatomy, microstructure and cutting-edge design-based stereology. The results of this study may shed light on the

* Corresponding author. Departamento de Cirurgia, Faculdade de Medicina Veterinária e Zootecnia, Universidade de São Paulo, Av. Prof. Dr. Orlando Marques de Paiva, 87, CEP 05508-270, São Paulo, SP, Brazil. Tel.: +55 11 3091 1214; fax: +55 11 3032 2224.
E-mail address: guto@usp.br (Ribeiro).

0736-5748/$36.00 © 2009 ISDN. Published by Elsevier Ltd. All rights reserved.
doi:10.1016/j.ijdevneu.2009.03.006

structural aspects of sympathetic ganglion neurons during post-natal development. In addition, these rodents may turn into a suitable animal model for studying the developing sympathetic nervous system, since they fall into a body-size category which places them between widely studied mice and rats and large wild rodents such as pacas and capybaras (Wilson and Reeder, 2005).

2. Materials and methods

2.1. Animals

Twenty right SCGs from 20 male guinea pigs (*Cavia porcellus* var. *albina*) were obtained from the animal-breeding company: *Biotério Itupeva – Produção de Animais para Pesquisa Ltda. EPT* (in São Paulo, Brazil). Guinea pigs were bred in plastic cages, whose dimensions were 100 cm× 66 cm × 30 cm, and in groups of five animals, which were fed on pellets of Nutricobaia (Purina®) and water *ad libitum*.

Based upon sexual maturation and the phases of post-natal development (Murphey and Olsen, 1994; Abrahão et al., 2009) animals were divided into four age groups ($N = 5$). Group 1: newborn (7 days old, mean BW: 163 g), group 2: young (30 days old, mean BW: 181 g), group 3: adult (7 months old, mean BW: 843 g) and group 4: old animals (50 months old, mean BW: 1.04 kg).

2.2. Methods

2.2.1. Histology

Animals were sedated with azaperone (Bayer®) (2 mg kg^{-1}, IM) followed by atropine sulphate (Bayer®) (0.06 mg kg^{-1}, IM). For the anaesthesia, a combination of ketamine chloride (Bayer®) (10 mg kg^{-1}, IM) and xylazine hydrochloride (Bayer®) (1.5 mg kg^{-1}, IM) was used, and the euthanasia procedure was conducted using an overdose of sodium pentobarbital (Bayer®) (100 mg kg^{-1}, IP).

A bulbed cannula was inserted into the left ventricle and a cleaning solution of phosphate-buffered saline (PBS) (0.1 M; pH 7.4) (Sigma®) containing 2% heparin (Roche®) and 0.1% sodium nitrite (Sigma®) was injected into the ascending aorta, and followed by a perfusion-fixation with a modified Karnovsky solution (5% glutaraldehyde and 1% formaldehyde) in a sodium cacodylate buffer (0.125 M; pH 7.4) (EMS®). Right SCGs were then dissected out, weighed and their wet weights were converted into volumes, using a tissue density of 1.06 g cm^{-3}, for estimating tissue deformation (shrinkage). In addition, SCG thickness, width and length were measured using a digital pachymeter (Digimess®).

Subsequently, the SCGs' wet weights were converted into volumes to estimate the tissue shrinkage using a tissue density of 1.06 g cm^{-3}. The latter was estimated in three right SCGs per age group in a pilot study by simply weighing the SCGs and dividing their wet weights (g) (after perfusion-fixation) by their volumes (cm^3) estimated by liquid displacement (Scherle, 1970). Mean tissue densities and their coefficients of variation (CVs) were 1.059 g cm^{-3} (0.10) (newborn), 1.061 g cm^{-3} (0.09) (young), 1.060 g cm^{-3} (0.10) (adult) and 1.061 g cm^{-3} (0.10) (aged). Since inter-group differences did not attain significance ($N = 3$, $F = 1.7$, d.f. = 3.8, $p = 0.44$), the same tissue density, i.e. 1.06 g cm^{-3} was used for all age groups for estimating tissue shrinkage (see volume of ganglion for methodological details).

In order to produce vertical and uniform random sections (VUR sections) right SCGs were rotated along their own length by means of a bar rotator and their vertical axes were marked using a Tissue Marking Dye System (Cancer Diagnostics, INC®). SCGs were embedded in a 7% agar solution, and using a tissue slider, they were systematically, uniformly and randomly cut into 0.5 mm-thick slabs generating four, five, seven and seven slabs in newborn, young, adult and old guinea pigs, respectively.

Subsequently, right SCGs were washed in a sodium cacodylate buffer, post-fixed in a solution of 2% osmium tetroxide in a sodium cacodylate buffer, stained en bloc with an aqueous solution saturated with uranyl acetate (EMS®), dehydrated in graded ethanol concentrations and propylene oxide (EMS®) and embedded in Araldite 502 EMS®. Specimens were polymerised in the oven at 60–70 °C for 3 days. For light microscopy, 0.4 and 2 μm-thick semi-thin sections were cut with glass knives, collected onto glass slides, dried on a hot plate, stained with toluidine blue and mounted under a coverslip with a drop of Araldite. Section images were acquired using a Leica® DMR microscope equipped with a DFC 300 FX Leica® Digital Camera and projected on a flat computer monitor. It has to be stressed that the identification of binucleate neurons was based upon counting the total number of nuclei per neuron using serial sections, and not only a single section.

2.3. Stereology (design-based)

A modification of the physical disector (Gundersen, 1986) was used in this present study. The approach used, which comprised a reference and two look-up sections including a stack of serial sections between them, was adopted to ensure the correct identification and sampling of mononucleate and binucleate neurons. Cell nucleoli were sampled to estimate the perikaryon volume (see mean volume of mononucleate and binucleate neurons) and the second look-up section, which is further apart from the first look-up section, was used to sample the perikarya and estimate the total number of SCG neurons.

2.4. Numerical density of mononucleate and binucleate neurons: N_v (mononuc, SCG) and N_v (binuc, SCG).

A modified physical disector was used to estimate the numerical density. The method consists in counting the number of neurons that are present within unbiased counting frames on reference sections, which do not touch either the forbidden lines of the frames or their extensions and disappear on subsequent look-up sections.

The formula for N_v estimation is: $N_v = \sum Q^-(\text{SCG cell})/\sum V(\text{SCG})$ where $\sum Q^-$ represents the cell count and $\sum V(\text{SCG})$ is the volume of all disectors sampled. The latter is estimated as $\sum P(a{:}p)h$, where P is the number of test points, $(a{:}p)$ the area associated with each test point and h is the distance between disector planes (disector height). Unbiased counting frames (frame area = 38,100 μm^2) (Gundersen, 1977) were SUR superimposed on section fields of view and the same sampled area was followed towards six consecutive sections, i.e. one 2 μm-thick section followed by another 0.4 μm-thick section and four 2 μm-thick sections. Hence, two disector heights were produced, i.e. 0.4 μm for the nucleolus sampling and 8.4 μm for the perikaryon sampling. Disectors were SUR applied in all SCG slabs (Gundersen et al., 1999).

2.5. Volume of ganglion: V(SCG)

The total volume of SCG was estimated by means of the Cavalieri principle. Briefly, SCG Araldite-embedded blocks were exhaustively and serially sectioned and every 300th section ($K = 300$) was sampled and measured for cross-sectional area. The volume estimation was performed in a fraction ($F_n = 2^{-1}$) of the reference sections used for disectors. Then, $V(\text{SCG}) = \sum Pa(p)K\text{MA}$, where P is the number of test points hitting the whole reference space ($p = 250$ in newborn and young guinea pigs and 300 in adult and old guinea pigs), $a(p)$ is the area associated with each test point ($a(p) = 98{,}758\ \mu m^2$) and MA is the microtome advance (MA = 0.4 or 2 μm).

2.6. Total number of mononucleate and binucleate neurons: N (mononuc, SCG) and N (binuc, SCG).

The total number of SCG neurons (N) (both mononucleate and binucleate) was estimated by multiplying N_v by SCG volume ($V(\text{SCG})$): $N = N_v V(\text{SCG})$.

2.7. Volume density of mononucleate and binucleate neurons and their processes: V_v (mononuc, SCG) and V_v (binuc, SCG), and of the non-neuronal tissue: neuropil (V_v (neuropil, SCG)) and capillaries (V_v (cap, SCG))

The fractional volume of SCG occupied by mononucleate and binucleate neurons and their processes, and the one occupied by neuropil and capillaries was estimated by point counting in the same sections and employing the same number of points used for the Cavalieri estimate. By estimating the volume fraction of the SCG occupied by mono and binucleate neurons we have not only assessed the perikaryon (soma), but also perikaryal processes and the neuron glial capsule, which are very close to the soma and are, therefore, hit by the lattice of points used for estimating the volume density or volume fraction. A SUR sampling of fields was elicited and test points were randomly superimposed on a computer monitor. We counted the total number of points falling within the SCG $\sum P(\text{SCG})$ and the total number of points falling on neurons (and their processes), neuropil and capillaries ($\sum P(\text{SCG})$ neurons, neuropil, cap). Volume density was therefore estimated as: $V_v = \sum P(\text{SCG})$ neurons, neuropil, cap: $\sum P(\text{SCG})$.

2.8. Total volume of mononucleate and binucleate neurons: V (mononuc, SCG) and V (binuc, SCG), and of the non-neuronal tissue: neuropil (V (neuropil, SCG)) and capillaries (V (cap, SCG))

The total volume occupied by mono and binucleate neurons and their processes in the SCG, and occupied by neuropil and capillaries was indirectly estimated by multiplying their fractional volumes by the total volume of SCG, $V(\text{SCG})$ (Lima et al., 2007).

2.9. Mean volume of mononucleate and binucleate neurons: $\bar{v}_N$ (mononuc, SCG) and $\bar{v}_N$ (binuc, SCG).

The mean perikaryal volume of both mono and binucleate neurons was estimated by the Nucleator method (Gundersen, 1988) in the same reference sections used for numerical density estimation. Nucleoli were sampled using one 2 μm and one 0.4 μm-thick sections in a physical disector. For mononucleate neurons on average 107 cells were measured for newborn and young, and 104 cells for adult and old guinea pigs. For binucleate neurons on average 105 cells were measured for newborn and young, and 104 cells for adult and old guinea pigs. The following formula was used to estimate the neuron size: $\bar{v}_N = \sum(4\pi/3)_n{}^3$, where: $_n{}^3$ is the mean cubed distance from a cell's central point (nucleolus) to its boundaries. Distances between the cell's central point and its boundaries were measured with a calibrated ruler with classes of size superimposed on a plane computer screen (Sorensen, 1991) (Fig. 1).

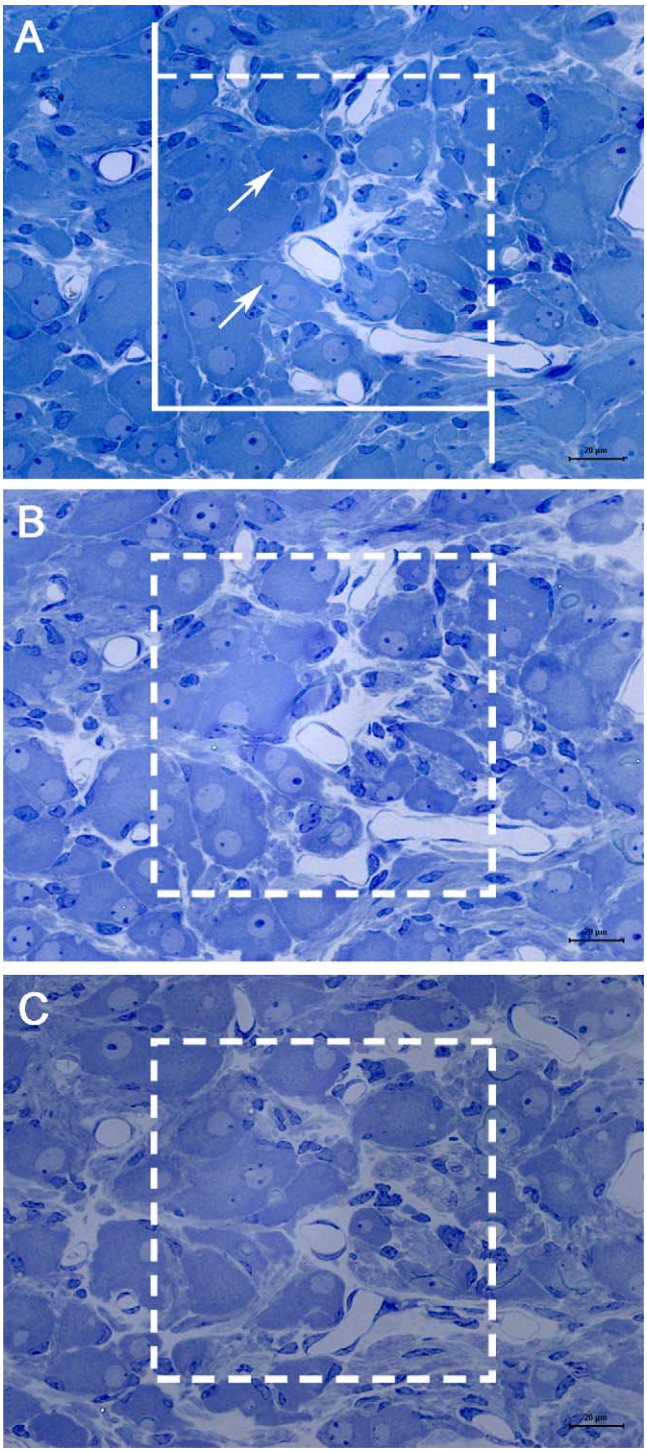

Fig. 1. An example of two disector-sampled neurons used for perikaryal neuronal volume (nucleator method) and number estimations. The reference section (A) and look-up 1 section (B) are separated by a height of 0.4 μm and reference section (A) and look-up 2 section (C) are separated by a height of 8.4 μm. In (A) the upper white arrow shows a neuronal cell body profile which is no longer present in the look-up 2 section (C). The lower white arrow in (A) shows a neuronal nucleolus profile which disappears in the look-up 1 section (B) and was, therefore, sampled for neuronal volume estimation. Toluidine blue. Scale bars: 20 μm.

2.10. Statistical analysis

Inter-group differences were assessed using one-way ANOVA through Minitab 15® (2007). When significant inter-group differences ($p < 0.05$) were noted a Tukey's test, corrected for simultaneous confidence intervals of 95%, was applied for multiple comparisons (level of significance $\alpha = 0.0126$). In addition, a Bonferroni-corrected Pearson's product-moment correlation was used to test the interrelation between animal body weight and the total number and size of mono and binucleate neurons or between animal body weight and ganglion volume, and the interrelation between ganglion volume and the total number and size of mono and binucleate neurons or between ganglion volume and animal body weight. Data were significant when $p < 0.00238$ (Kutner et al., 2005).

Results are shown as mean (CV_{obs}) (Shay, 1975; Nicholson, 1978; Gundersen and Østerby, 1980), where the observed total coefficient of variation (CV_{obs}) equals SD/mean. Additionally, Pearson's correlation data are given as coefficients of correlation (ρ) followed by their p-values (p), respectively.

3. Results

3.1. Anatomy

In all animals, irrespective of age, the right SCGs were roughly spindle-shaped and located in the most cranial part of the neck. Dorsally, the ganglia were in contact with the vagus nerve and, ventrally, they were close to the occipital artery. The caudal pole of SCG continued into the cervical sympathetic trunk. In newborn guinea pigs, SCG width, length and thickness were 1.11 mm (0.07), 2.25 mm (0.33) and 0.63 mm (0.17). In young animals, the values were: 0.99 mm (0.22), 2.70 mm (0.04) and 0.67 mm (0.05). In adult guinea pigs, the figures were: 1.58 mm (0.31), 3.70 mm (0.21) and 0.79 mm (0.11) and, finally, in old guinea pigs, the figures were 1.45 mm (0.17), 3.83 mm (0.18) and 1.05 mm (0.40). Differences amongst groups were significant ($N = 5$, $F = 9.85$, d.f. = 3.16, $p = 0.001$) for ganglion length, between newborn and old guinea pigs, but they were not significant for ganglion thickness ($N = 5$, $F = 1.38$, d.f. = 3.16, $p = 0.8$) and width ($N = 5$, $F = 1.40$, d.f. = 3.16, $p = 0.7$).

3.2. Microstructure

In semi-thin sections, the right SCG consisted of clusters of neurons separated by nerve fibres, blood vessels and prominent septa of connective tissue. Ganglion neuron profiles were circular or oval-shaped. SCG neurons were densely distributed and packed in newborn animals (Fig. 2A). In old guinea pigs, SCG neurons were separated by spaces mainly occupied by non-neuronal tissue (Fig. 2B). Regardless of animal age, in mononucleate neurons, nuclei were located either in the centre of the perikaryon or eccentrically. On the other hand, in binucleate neurons the nuclei occupied the two poles of the cell having a very distinct and defined position within the cell (Fig. 2A–C).

3.3. Stereology

3.3.1. Numerical density of mononucleate and binucleate neurons: N_v (mononuc, SCG) and N_v (binuc, SCG)

For mononucleate neurons, on average 46 disectors were used to count 127 cells in newborn, 54 disectors to count 110 cells in young, 67 disectors to count 112 cells in adult and 76 disectors to count 107 cells in old guinea pigs. The mean number of disectors applied per SCG slab was 11, 10, 9 and 10 in newborn, young, adult and old guinea pigs, respectively. For binucleate neurons, on average 70 disectors were used to count 110 cells in newborn, 84 disectors to count 107 cells in young, 95 disectors to count 113 cells in adult and 107 disectors to count 114 cells in old guinea pigs. The mean number of disectors applied per SCG slab was 17, 16, 13 and 15 in newborn, young, adult and old guinea pigs, respectively.

The numerical density of mononucleate neurons was 51,410 mm^{-3} (0.01) in newborn, 48,301 mm^{-3} (0.04) in young, 36,551 mm^{-3} (0.07) in adult and 34,040 mm^{-3} (0.04) in old guinea pigs. Significant differences were noted between newborn and adult, newborn and old, young and adult, and between young and old guinea pigs ($N = 5$, $F = 65.07$, d.f. = 3.16, $p = 0.001$). The numerical density of binucleate neurons was 11,226 mm^{-3}

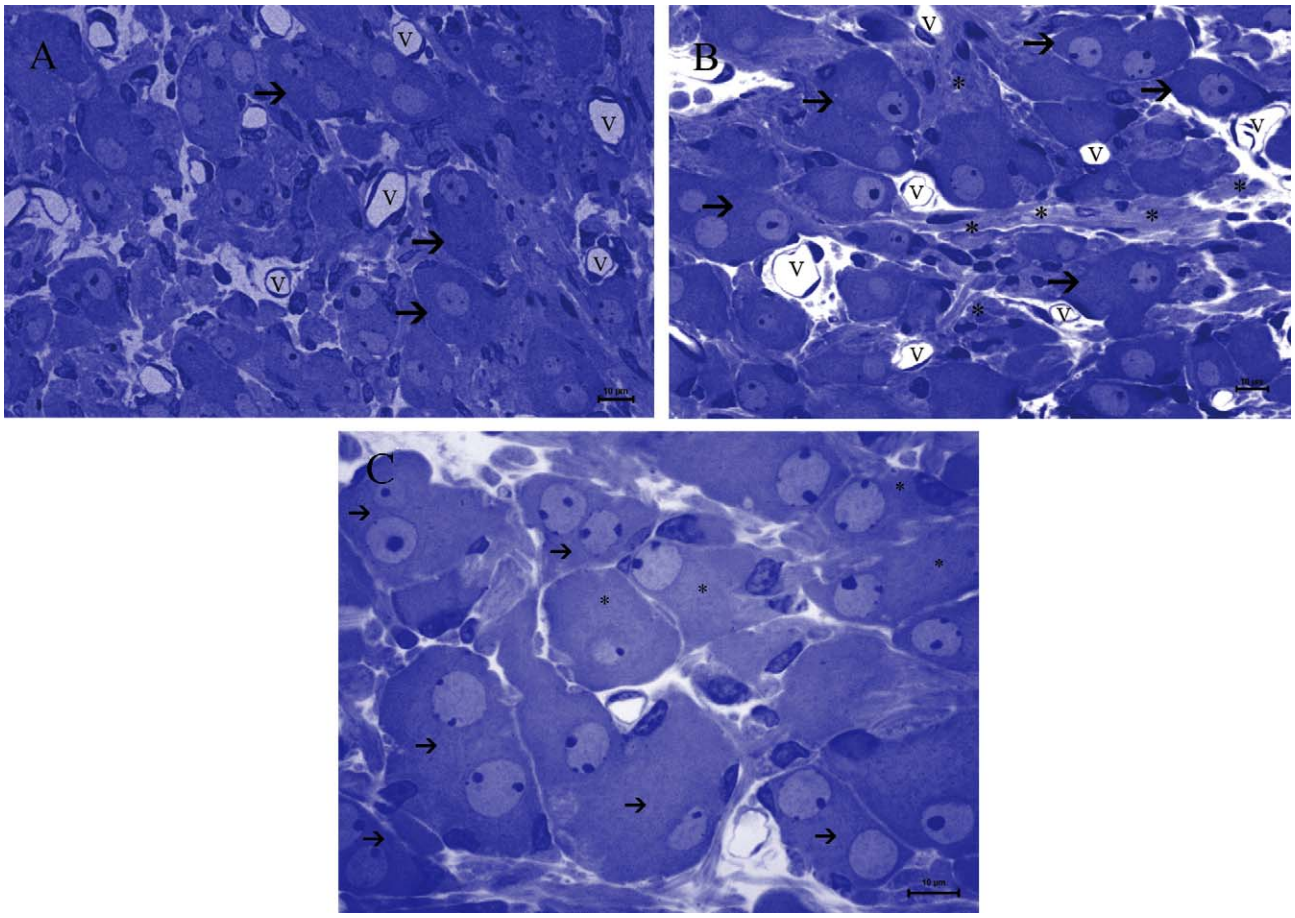

Fig. 2. Structure of the superior cervical ganglion of a newborn (A) and old guinea pig (B) in semi-thin sections (2 μm) at the same magnification. Mono and binucleate neurons (arrows) were densely distributed and packed in newborn animals, and separated by intra-ganglionic vessels (v). However, in the old guinea pig (B) mono and binuleate neurons (arrows) were separated by large spaces mainly occupied by non-neuronal tissue (*) as well as vessels (v). Toluidine blue. Scale bars: 10 μm. (C) The right SCG (adult guinea pig) in semi-thin sections (2 μm) depicting structural differences between mono (*) and binucleate neurons (arrows). In mononucleate neurons, the nuclei were mostly eccentric, whereas in binucleate neurons the nuclei occupied the two poles of the cell having a very distinct and defined position within the cell. Toluidine blue. Scale bar: 10 μm.

(0.22) in newborn, 9269 mm^{-3} (0.06) in young, 6196 mm^{-3} (0.16) in adult and 5040 mm^{-3} (0.01) in old guinea pigs. Differences between groups were significant, i.e. between newborn and adult, newborn and old, young and adult, young and old, and between adult and old guinea pigs ($N = 5$, $F = 64.10$, d.f. = 3.16, $p = 0.002$).

3.4. Volume of ganglion: V(SCG)

The global shrinkage on SCG volume (%) was 7.95 (0.15) in newborn, 7.56 (0.20) in young, 7.47 (0.18) in adult and 7.43 (0.18) in old guinea pigs. No correction for global shrinkage was applied since inter-group differences were not statistically significant ($N = 5$, $F = 2.17$, d.f. = 3.16, $p = 0.4$). SCG volume was 3.99 mm^3 (0.04) in newborn, 4.65 mm^3 (0.06) in young, 5.59 mm^3 (0.09) in adult and 5.05 mm^3 (0.09) in old guinea pigs. Differences amongst groups were significant, i.e. between newborn and adult, and between newborn and old guinea pigs ($N = 5$, $F = 23.17$, d.f. = 3.16, $p = 0.006$) (Fig. 3). The error variance of the Cavalieri estimate (CE(VSCG)) was 0.02 for newborn, 0.03 for young, 0.03 for adult and 0.04 for old guinea pigs.

3.5. Total number of mononucleate and binucleate neurons: N (mononuc, SCG) and N (binuc, SCG)

The total number of mononucleate neurons was 205,413 (0.03) in newborn, 224,285 (0.03) in young, 204,433 (0.13) in adult and 171,503 (0.06) in old guinea pigs. Differences amongst groups were significant, i.e. between young and old guinea pigs ($N = 5$, $F = 20.92$, d.f. = 3.16, $p = 0.017$) (Fig. 4A). The total number of binucleate neurons was 44,617 (0.19) in newborn, 43,062 (0.06) in young, 34,457 (0.14) in adult and 25,456 (0.10) in old guinea pigs. Differences between groups were significant, i.e. between newborn and old, and between young and old guinea pigs ($N = 5$, $F = 28.55$,

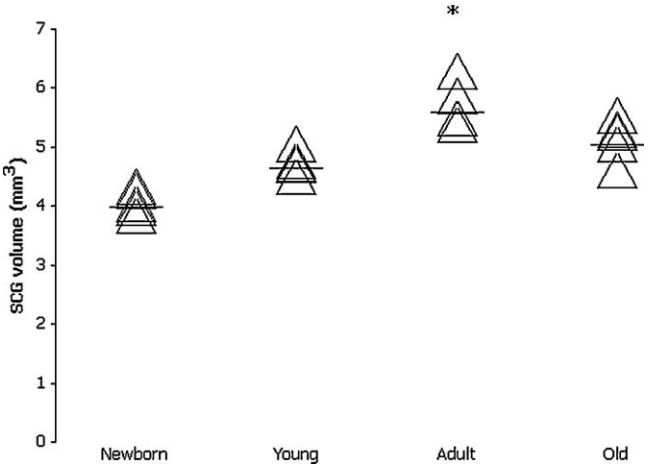

Fig. 3. SCG volume of guinea pigs during post-natal development. There were significant differences amongst age groups (*$p = 0.006$). Triangles indicate individual values and horizontal bars show group means.

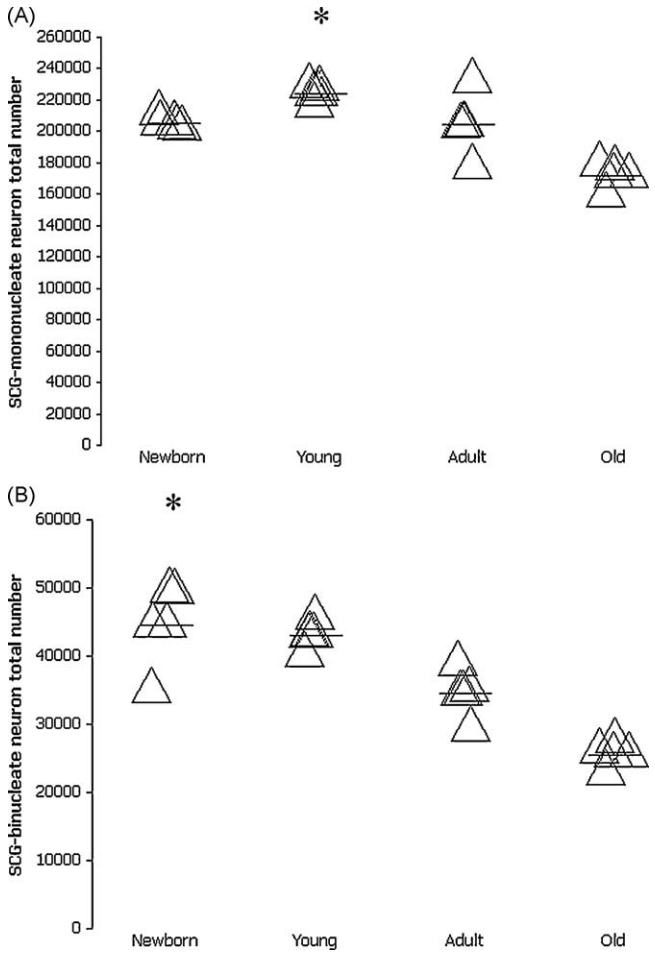

Fig. 4. (A) SCG-mononucleate neuron total number and (B) SCG-binucleate neuron total number. Inter-group differences were significant for both mononucleate (*$p = 0.017$) and binucleate (*$p = 0.007$) neurons. Triangles indicate individual values and horizontal bars show group means.

d.f. = 3.16, $p = 0.007$) (Fig. 4B). For mononucleate neurons the error variance of this estimate (CE(N)) was 0.08 for newborn, 0.11 for young, 0.12 for adult and 0.14 for old guinea pigs, respectively. For binucleate neurons CE(N) was 0.05 for newborn, 0.08 for young, 0.09 for adult and 0.13 for old guinea pigs, respectively.

3.6. Volume density of mononucleate and binucleate neurons and their processes: V_v (mononuc, SCG) and V_v (binuc, SCG), and of the non-neuronal tissue: neuropil (V_v (neuropil, SCG)) and capillaries (V_v (cap, SCG))

The volume density of mononucleate neurons and their processes was: 0.28 (0.02) in newborn, 0.24 (0.06) in young, 0.20 (0.06) in adult and 0.19 (0.02) in old guinea pigs. Differences amongst groups were significant, i.e. between newborn and young, newborn and adult, newborn and old, young and adult, and between young and old guinea pigs ($N = 5$, $F = 173.78$, d.f. = 3.16, $p = 0.001$). The volume density of binucleate neurons and their processes was: 0.06 (0.18) in newborn, 0.04 (0.13) in young, 0.04 (0.16) in adult and 0.03 (0.01) in old guinea pigs. Differences amongst groups were significant, i.e. between newborn and young, newborn and adult, and between newborn and old guinea pigs ($N = 5$, $F = 23.17$, d.f. = 3.16, $p = 0.002$). The volume density of the neuropil was: 0.60 (0.03) in newborn, 0.68 (0.24) in young, 0.74 (0.13) in adult and 0.76 (0.19) in old guinea pigs. Differences amongst groups were significant, i.e. between newborn and adult, and between newborn and old guinea pigs ($N = 5$, $F = 228.97$, d.f. = 3.16, $p = 0.003$). The volume density of the capillaries was: 0.06 (0.05) in newborn, 0.04 (0.18) in young, 0.02 (0.10) in adult and 0.02 (0.17) in old guinea pigs. Differences amongst groups were significant, i.e. between newborn and adult and between newborn and old guinea pigs ($N = 5$, $F = 22.24$, d.f. = 3.16, $p = 0.001$).

3.7. Total volume of mononucleate and binucleate neurons: V (mononuc, SCG) and V (binuc, SCG), and of the non-neuronal tissue: neuropil (V (neuropil, SCG)) and capillaries (V (cap, SCG))

The total volume occupied by mononucleate neurons and their processes in the SCG was 1.1172 mm^3 (0.04) in newborn, 1.116 mm^3 (0.03) in young, 1.118 mm^3 (0.10) in adult and 0.9595 mm^3 (0.12) in old guinea pigs. Differences amongst groups did not attain statistical significance ($N = 5$, $F = 9.85$, d.f. = 3.16, $p = 0.095$) (Fig. 5A). The total volume occupied by binucleate neurons and their processes in the SCG was 0.2394 mm^3 (0.15) in newborn, 0.186 mm^3 (0.10) in young, 0.2236 mm^3 (0.06) in adult and 0.1515 mm^3 (0.07) in old guinea pigs. Differences between groups were significant between newborn and old guinea pigs ($N = 5$, $F = 31.42$, d.f. = 3.16, $p = 0.005$) (Fig. 5B). The total volume of the neuropil was: 2.394 mm^3 (0.14) in newborn, 3.162 mm^3 (0.27) in young, 4.1366 mm^3 (0.14) in adult and 3.838 mm^3 (0.17) in old guinea pigs. Differences amongst groups were significant between newborn and adult, and between newborn and old guinea pigs ($N = 5$, $F = 223.17$, d.f. = 3.16, $p = 0.001$). The total volume occupied

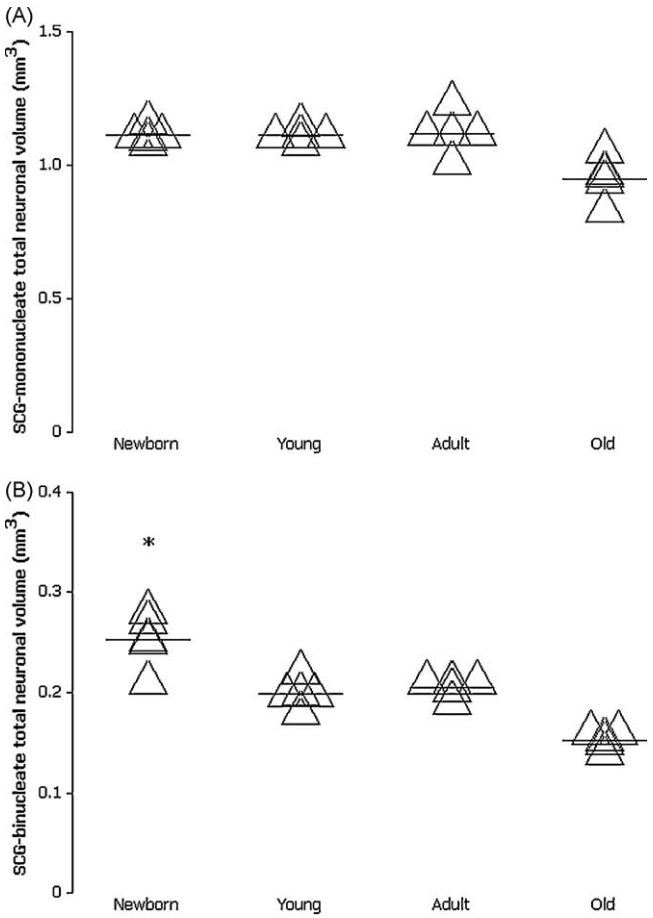

Fig. 5. (A) Total volume of mononucleate neurons and (B) total volume of binucleate neurons in the guinea pig's SCG during post-natal development. Inter-group differences did not attain statistical significance for mononucleate ($p = 0.095$), but reached significance for binucleate neurons (*$p = 0.005$). Triangles indicate individual values and horizontal bars show group means.

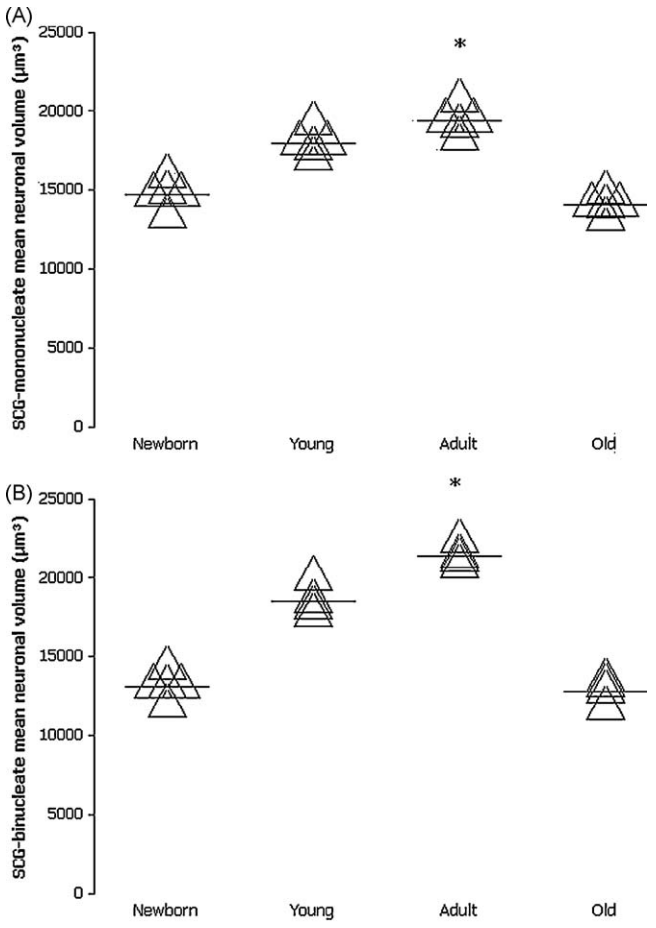

Fig. 6. (A) SCG-mononucleate mean neuron volume and (B) SCG-binucleate mean neuron volume. There were significant inter-group differences for both mononucleate (*$p = 0.001$) and binucleate (*$p = 0.001$) neurons. Triangles indicate individual values and horizontal bars show group means.

by capillaries was: 0.2394 mm^3 (0.14) in newborn, 0.186 mm^3 (0.16) in young, 0.1118 mm^3 (0.11) in adult and 0.101 mm^3 (0.27) in old guinea pigs. Differences amongst groups were significant, i.e. between newborn and adult, and between newborn and old guinea pigs ($N = 5$, $F = 34.17$, d.f. = 3.16, $p = 0.02$).

3.8. Mean volume of mononucleate and binucleate neurons: $\bar{v}_N$ (mononuc, SCG) and $\bar{v}_N$ (binuc, SCG)

The mean perikaryal volume of mononucleate neurons was 14,742 μm^3 (0.09) in newborn, 18,001 μm^3 (0.06) in young, 19,396 μm^3 (0.06) in adult and 14,062 μm^3 (0.06) in old guinea pigs (Fig. 6A). For binucleate neurons the figures were 13,151 μm^3 (0.09) in newborn, 18,590 μm^3 (0.07) in young, 21,429 μm (0.04) in adult and 12,851 μm^3 (0.07) in old guinea pigs (Fig. 6B). Differences amongst groups were significant for mononucleate neurons, i.e. between newborn and young, newborn and adult, young and old, and between adult and old guinea pigs ($N = 5$, $F = 51.51$, d.f. = 3.16, $p = 0.001$). For binucleate neurons the figures were significant, i.e. between newborn and young, newborn and adult, young and adult, young and old, and between adult and old guinea pigs ($N = 5$, $F = 159.32$, d.f. = 3.16, $p = 0.001$).

3.9. Correlation between variables

Significant high-intensity positive correlations were seen between animal body weight and the mean perikaryal volume of binucleate neurons ($\rho = 0.82$; $p = 0.001$), and between the mean perikaryal volumes of mono and binucleate neurons ($\rho = 0.92$; $p = 0.001$). In addition, a significant high-intensity negative correlation was seen between animal age and the total number of binucleate neurons ($\rho = -0.84$; $p = 0.001$).

4. Discussion

The main findings of this study were a combination of post-natal-dependent increases and decreases in some structural parameters of SCG: (i) 27% increase in ganglion volume, (ii) 24% and 43% decreases in the total number of mono and binucleate neurons, respectively, and (iii) 27.5% and 40% decreases in the mean perikaryal volume of mono and binucleate neurons, respectively.

4.1. Qualitative microstructure

Irrespective of age, all SCGs were enveloped by a connective capsule, which sent septa of connective tissue inside the ganglia, dividing them into several ganglion units. This general pattern is in line with previous qualitative studies focusing on the sympathetic ganglia of several large mammals such as dogs, horses, cats (Ribeiro et al., 2002; Gagliardo et al., 2003 and Fioretto et al., 2007), rabbits (Sasahara et al., 2003) and capybaras (Ribeiro et al., 2004 and Ribeiro, 2006).

4.2. Stereology

Hypertrophy is a widely known adaptive mechanism during post-natal development in most autonomic ganglia from medium-sized to large mammals (Gagliardo et al., 2005; Miolan and Niel, 1996 and Fioretto et al., 2007). As with previous studies (Ribeiro et al., 2004; Gagliardo et al., 2005 and Ribeiro, 2006) guinea pig post-natal development was marked by a 27% increase in the SCG volume, which was accompanied by a 538% increase in the animal body weight. However, in addition to nervous tissue ganglia contain a noticeable amount of non-neuronal tissue, i.e. connective tissue and blood vessels. The differences in ganglion volume may partially reflect a variation in the total volume of the nervous tissue, and partially a variation in the vascular and connective tissue total volumes due to a possible functional overload triggered by the ganglion's target-organ's growth during post-natal development. Indeed, although the total volume of binucleate neurons decreased by 40%, the ganglion volume increased by 27%. On the contrary, there were no changes in the total volume occupied by mononucleate neurons in the same SCG, albeit their fractional volume decreased by 32% during the post-natal developmental period. This phenomenon confirms that conclusions based only upon ratios are generally misleading due to the reference trap, which happens when there is a dearth of knowledge of the reference volume (SCG volume) (Braendgaard and Gundersen, 1986; Hunziker and Cruz-Orive, 1986; Cruz-Orive, 1994; Nyengaard, 1999; Mayhew, 2008).

Another striking finding of this study was a 24% and 43% ageing-induced decrease in the total number of mononucleate and binucleate SCG neurons, respectively. The loss of binucleate SCG neurons (43%) matched the reduction in the total volume occupied by the same binucleate neurons in the SCG, i.e. 40%. Indeed, a high-intensity negative correlation was found between animal age and the total number of binucleate neurons, i.e. the older the animal the lower the number of binucleate SCG neurons. By the same token, Ribeiro (2006) found a 23% decrease in the total number of binucleate SCG neurons in capybaras during maturation. A similar neuronal number reduction was also reported by Bergman and Ulfhake (1998), when comparing DRG with 30-day-old and 3-month-old rats. Santer (1991) also described a decrease in the total

number of neurons in SCG between 4 and 24-month-old rats. Neuron loss during ageing has also been attributed to a decrease in the production of neuroactive steroids, i.e. dehydroepiandrosterone sulphate ester and allopregnanolone, which are inhibitors of neuron apoptosis that occurs during ageing, and which protect CNS and sympathetic neurons from noxious agents (Charalampopoulos et al., 2006).

Although a fall in neuron numbers seems a common pattern during post-natal development, Farel (2003) reported an increase in the number of neurons in the DRG of rats, which was not associated with a possible neurogenesis, but perhaps, with late maturation or incomplete differentiation. On the contrary, recent publications describing binucleate neurons in the SCG of adult wild rodents such as capybaras (Ribeiro et al., 2004; Ribeiro, 2006) and in the coeliac ganglion of adult lagomorphs (rabbits) (Sasahara et al., 2003), add further fuel to the notion that a post-natal neurogenesis may indeed exist in sympathetic ganglia. In effect, a larger number of hypogastric ganglion neurons was reported by Warburton and Santer (1997) in rats of 24 months compared to rats of 4 months, in the number of DRG neurons of 80-day-old rats compared with 11-day-old rats (Popken and Farel, 1997), and in the number of caudal mesenteric ganglion (CMG) neurons of middle-aged dogs compared to young dogs (a 17-fold increase) (Gagliardo et al., 2005).

Concerning post-natal-induced changes, some parts of the nervous system may react differently and the reasons for this are still unclear. For example, in the CNS, the most frequent reported changes are neocortical neuron loss, atrophy of remaining neurons (Esiri, 2007) and loss of both Purkinje and granular cells in the anterior lobe of cerebellum (Andersen et al., 2003) and dopaminergic cells in the substantia nigra (Sanchez et al., 2008). Again, these findings are controversial because there are differences between various components of the nervous system and also among animal species (Finch, 1993; Vega et al., 1993). Additionally, differences in the sizes of ganglion neurons are somehow related to body weight and organ weight ranges, the largest species or organs having the largest sizes of neurons, though they are obviously not proportional to organ or body weight variations (Purves et al., 1986b). Mayhew (1991) using a direct design-based stereological number estimator, i.e. the physical fractionator, showed that the weight of the mammalian cerebellum affords a satisfactory way of predicting the total number of Purkinje cells. Furthermore, Gagliardo et al. (2005) reported that the dog's body weight as well as the CMG volume, allowed for an accurate prediction of the total number of CMG neurons.

A third and unexpected finding of this study was the atrophy of mono (27.5%) and binucleate (40%) SCG neurons during the ageing phase of post-natal development, i.e. from adult to old subjects. Our results contrast starkly with previous studies in literature, in which an ageing-induced neuron hypertrophy happens to be a common event, at least in the CNS, to compensate for a neuron loss in the same period (Cabello et al., 2002). For instance, neuron volume increased by 217% in the dog's CMG during maturation and ageing (Gagliardo et al., 2005). By contrast, we found no correlation between neuron size and animal age, though we did see a high-intensity positive correlation between the size of binucleate neurons and animal body weight. Remarkably, there was also a 92.4% high-intensity positive correlation between the sizes of mono and binucleate neurons, i.e. the smaller (or higher) the mononucleate neuron the smaller (or higher) the binucleate neuron. A possible explanation for this unexpected post-natal neuron atrophy might be, as suggested by Al-Shawi et al. (2008), a selective age-related atrophy and neurodegeneration mediated by an increase in the sortilin expression in SCG neurons, together with elevated expression of proNGF levels in some targets. Thus, the chances are that alternative neuron-size regulating mechanisms, apart from hypertrophy, may be acting or co-acting during post-natal development.

5. Conclusions and remarks for further studies

At the time of writing there are still no functional explanations underlying the quantitative structural changes in the guinea pig's SCG during post-natal development. Since the target tissue increases in volume and surface area, the number of ganglion neurons would then increase as a function of the quantity of target tissue innervated by them (Ebbesson, 1968a), though it was not currently seen in the guinea pig's SCG. However, having a heterogeneous population of nerve cells, e.g. secretomotor, pilomotor or vasomotor neurons, SCG neurons may be subjected to differential structural changes depending upon the organs they target, i.e. neurons innervating the iris have the largest cell bodies and most extensive dendritic arborizations, whereas the vasomotor neurons are the smallest (Andrews et al., 1996). Neurons innervating the middle cerebral artery (MCA) halt dendritic growth early in post-natal development, whereas the dendritic complexity of neurons supplying the submandibular gland increases well into adulthood (Andrews et al., 1996). We therefore suggest that forthcoming mechanistic studies on sympathetic ganglia should investigate whether age-related changes preferentially target a neuron population; this could be achieved by labelling neurons with specific markers, e.g. neuropeptide Y (NPY).

Another interesting investigation field would be the interaction between ganglion neurons, their innervation targets and the signalling growth factors produced by the latter. Would the differences in the sizes of the innervation targets and in the quality of the signals raised by the target organs explain the changes in the neuron structure during post-natal development?

Acknowledgment

The Laboratory of Stochastic Stereology and Chemical Anatomy (LSSCA) is supported by Fundação de Amparo à Pesquisa do Estado de São Paulo (FAPESP) (application number 05-02346-5).

References

Abrahão, L.M.B., Nyengaard, J.R., Sasahara, T.H.C., Gomes, S.P., Oliveira, F.R., Ladd, F.V.L., Ladd, A.A.B.L., de Melo, M.P., Machado, M.R.F., Melo, S.R., Ribeiro, A.A.C.M., 2009. Asymmetric post-natal development of superior cervical ganglion of paca (*Agouti paca*). Int. J. Dev. Neurosci. 27, 37–45.

Al-Shawi, R., Hafner, A., Olson, J., Chun, S., Raza, S., Thrasivoulou, C., Lovestone, S., Killick, R., Simons, P., Cowen, T., 2008. Neurotoxic and neurotrophic roles of proNGF and the receptor sortilin in the adult and ageing nervous system. Eur. J. Neurosci. 27, 2103–2114.

Andersen, B.B., Gundersen, H.J., Pakkenberg, B., 2003. Aging of the human cerebellum: a stereological study. J. Comp. Neurol. 466, 356–365.

Andrews, T.J., Thrasivoulou, C., Nesbit, W., Cowen, T., 1996. Target-specific differences in the dendritic morphology and neuropeptide content of neurons in the rat SCG during development and aging. J. Comp. Neurol. 368, 33–44.

Bergman, E., Ulfhake, B., 1998. Loss of primary sensory neurons in the very old rat: neuron number estimates using the dissector method and confocal optical sectioning. J. Comp. Neurol. 396, 211–222.

Braendgaard, H., Gundersen, H.J.G., 1986. The impact of recent stereological advances on quantitative studies of the nervous system. J. Neurosci. Methods 18, 39–78.

Cabello, C.R., Thune, J.J., Pakkenberg, H., Pakkenberg, B., 2002. Ageing of substantia nigra in humans: cell loss may be compensated by hypertrophy. Neuropathol. Appl. Neurobiol. 28, 283–291.

Charalampopoulos, I., Alexaki, V.I., Tsatsanis, C., Minas, V., Dermitzaki, E., Lasaridis, I., Vardouli, L., Stournaras, C., Margioris, A.N., Castanas, E., Gravanis, A., 2006. Neurosteroids as endogenous inhibitors of neuronal cell apoptosis in aging. Ann. N. Y. Acad. Sci. 1088, 139–152.

Cruz-Orive, L.M., 1994. Toward a more objective biology. Neurobiol. Aging 15, 377–378.

Ebbesson, S.O.E., 1968a. Quantitative studies of the superior cervical sympathetic ganglia in a variety of primates including man. J. Morphol. 124, 117–132.

Esiri, M., 2007. Ageing and the brain. J. Pathol. 211, 181–187.

Farel, P.B., 2003. Late differentiation contributes to the apparent increase in sensory neuron number in juvenile rat. Developmental. Brain Res. 144, 91–98.

Finch, C.E., 1993. Neuron atrophy during aging: programmed or sporadic? Trends Neurosci. 6, 104–110.
Fioretto, E.T., Abreu, R.N., Castro, M.F.S., Guidi, W.L., Ribeiro AACM, 2007. Macro and microstructure of the superior cervical ganglion in dogs, cats and horses during maturation. Cells Tissues Organs 186, 129–140.
Gagliardo, K.M., Silva, R.A., Guidi, W.L., Ribeiro AACM, 2003. Macro and microestructural organization of the dog's caudal mesenteric ganglion complex (*Canis familiaris*). Anatomia, Histologia, Embryologia 32, 236–243.
Gagliardo, K.M., Balieiro, J.C.C., Souza, R.R., Ribeiro AACM, 2005. Postnatal-related changes in the size and total number of neurons in the caudal mesenteric ganglion of dogs: total number of neurons can be predicted from body weight and ganglion volume. Anat. Rec. Part A 286A, 917–929.
Gundersen, H.J.G., 1977. Notes of the estimation of the numerical density of arbitrary profiles: the edge effect. J. Microsc. 111, 219–223.
Gundersen, H.J.G., 1986. Stereology of arbitrary particles. A review of unbiased number and size estimators and presentation of some new ones, in memory of William R. Thompson. J. Microsc. 143, 3–45.
Gundersen, H.J.G., 1988. The nucleator. J. Microsc. 151, 3–21.
Gundersen, H.J.G., Jensen, F.B., Kiev, K., Nielsen, J., 1999. The efficiency of systematic sampling in stereology – reconsidered. J. Microsc. 193, 199–211.
Gundersen, H.J.G., Østerby, R., 1980. Sampling efficiency and biological variation in stereology. Mikroskopie (Suppl. 37), 143–148.
Hunziker, E.B., Cruz-Orive, L.M., 1986. Consistent and efficient delineation of reference spaces for light microscopical stereology using a laser microbeam system. J. Microsc. 142, 95–99.
Kutner, M.H., Nachtsheim, C.J., Neter, J., Li, W., 2005. Applied Linear Statistical Models, 5th ed. McGraw-Hill Irwin, New York, p. 1396.
Lima, A.R., Nyengaard, J.R.N., Jorge, A.A.L., Balieiro, J.C.C., Peixoto, C., Fioretto, E.T., Ambrósio, C.E., Miglino, M.A., Zatz, M., Ribeiro, A.A.C.M., 2007. Muscular dystrophy-related quantitative and chemical changes in adenohypophysis GH-cells in Golden Retrievers. Growth Horm. IGF Res. 17, 480–491.
Mayhew, T.M., 1991. Accurate prediction of Purkinje cell number from cerebellar weight can be achieved with the fractionator. J. Comp. Neurol. 308, 162–168.
Mayhew, T.M., 2008. Taking tissue samples from the placenta: an illustration of principles and strategies. Placenta 29, 1–14.
Minitab (v.15) (2007) Minitab reference manual. Minitab Inc. State College, PA, USA.
Miolan, J., Niel, J., 1996. The mammalian sympathetic prevertebral ganglia: integrative properties and role in the nervous control of digestive tract motility. J. Auton. Nerv. Syst. 58, 125–138.
Murphey, L.J., Olsen, G.D., 1994. Morphine-6-beta-D-glucuronide respiratory pharmacodynamics in the neonatal guinea pig. J. Pharmacol. Exp. Ther. 271, 118–124.
Nicholson, W.L., 1978. Application of statistical methods in quantitative microscopy. J. Microsc. 113, 223–239.
Nyengaard, J.R., 1999. Stereologic methods and their application in kidney research. J. Am. Soc. Nephrol. 10, 1100–1123.
Popken, G.J., Farel, P.B., 1997. Sensory neuron number in the neonatal and adult rats estimated by means of the stereologic and profile-based methods. J. Comp. Neurol. 386, 8–15.
Purves, D., Rubin, E., Snider, W.D., Lichtman, J., 1986b. Relation of animal size to convergence, divergence and neuronal number in peripheral sympathetic pathways. J. Neurosci. 6, 158–163.
Ribeiro, A.A.C.M., Elias, C.F., Liberti, E.A., Guidi, W.L., De Souza, R.R., 2002. Structure and ultrastructure of the celiac-mesenteric ganglion complex in the domestic dog (*Canis familiaris*). Anat. Histol. Embryol. 31, 344–349.
Ribeiro, A.A.C.M., 2006. Size and number of binucleate and mononucleate superior cervical ganglion neurons in young capybaras. Anat. Embryol. (Berlin) 211, 607–617.
Ribeiro, A.A.C.M., Davis, C., Gabella, G., 2004. Estimate of size and total number of neurons in superior cervical ganglion of rat, capybara and horse. Anat. Embryol. 208, 367–380.
Sanchez, H.L., Silva, L.B., Portiansky, E.L., Herenu, C.B., Goya, R.G., Zuccolilli, G.O., 2008. Dopaminergic mesencephalic systems and behavioral performance in very old rats. Neuroscience 154, 1598–1606.
Santer, R.M., 1991. Sympathetic neurone numbers in ganglia of young and old rats. J. Auton. Nerv. Syst. 33, 221–222.
Sasahara, T.H.C., De Souza, R.R., Machado, M.R.F., Da Silva, R.A., Guidi, W.L., Ribeiro, A.A.C.M., 2003. Macro and microstructural organization of the rabbit's celiac-mesenteric ganglion complex. Ann. Anat. 185, 441–448.
Scherle, W., 1970. A simple method for volumetry of organs in quantitative stereology. Mikroskopie 26, 57–60.
Shay, J., 1975. Economy of effort in electron microscope morphometry. Am. J. Pathol. 81, 503–512.
Sorensen, F.B., 1991. Stereological estimation of the mean and variance of nuclear volume from vertical sections J. J. Microsc. 162, 203–229.
Vega, J.A., Calzada, B., Del Valle ME, 1993. Age-related in the mammalian autonomic and sensory ganglia. In: Amenta, F. (Ed.), Aging of the Autonomic Nervous System. CRC Press, London.
Warburton, A.L., Santer, R.M., 1997. The hypogastric ant thirteenth thoracic ganglia of the rat: effects of age on the neurons and their extracellular environment. J. Anat. 190, 115–124.
Wilson, D.E., Reeder, D.M., 2005. Mammal Species of the World: A Taxonomic and Geographic Reference, 3rd ed. Johns Hopkins University Press, Baltimore, Maryland, p. 2,142.